HYDROLOGICAL PROCESSES
Hydrol. Process. **18**, 107–123 (2004)
Published online 7 November 2003 in Wiley InterScience (www.interscience.wiley.com). DOI: 10.1002/hyp.1315

Correlation between El Niño–Southern Oscillation (ENSO) and precipitation in South-east Asia and the Pacific region

Z. X. Xu,[1,2]* K. Takeuchi[1] and H. Ishidaira[1]

[1] *Institute of Materials and Environmental Technology, Graduate School, Yamanashi University, Kofu, 400-8511, Japan*
[2] *Institute for Water Sciences, Beijing Normal University, Beijing 100875, P. R. China*

Abstract:

The relationship between El Niño–Southern Oscillation (ENSO) events versus precipitation anomalies, and the response of seasonal precipitation to El Niño and La Niña events were investigated for 30 basins that represent a range of climatic types throughout South-east Asia and the Pacific region. The teleconnection between ENSO and the hydroclimate is tested using both parametric and non-parametric approaches, and the lag correlations between precipitation anomalies versus the Southern Oscillation Index (SOI) several months earlier, as well as the coherence between SOI and precipitation anomalies are estimated. The analysis shows that dry conditions tend to be associated with El Niño in the southern zone, and part of the middle zone in the study area. The link between precipitation anomalies and ENSO is statistically significant in the southern zone and part of the middle zone of the study area, but significant correlation was not observed in the northern zone. Patterns of precipitation response may differ widely among basins, and even the response of a given river basin to individual ENSO events also may be changeable. Copyright © 2003 John Wiley & Sons, Ltd.

KEY WORDS El Niño–Southern Oscillation (ENSO); Southern Oscillation Index (SOI); El Niño; La Niña; precipitation

INTRODUCTION

Both variability and change from climate have direct impacts for social and economic activities, and therefore have been the subject of numerous studies in hydrology and water resources for many years. The El Niño–Southern Oscillation (ENSO) phenomenon, resulting from the interaction between large-scale ocean and atmospheric circulation processes in the equatorial Pacific Ocean, is one of the major factors influencing climate variations and has been linked to climate anomalies throughout the world. The ENSO itself constitutes a complex of environmental changes that have different influences throughout the globe, and are loosely associated, statistically and physically, with the major regional precipitation-generating mechanisms (Waylen and Poveda, 2002). A number of studies have demonstrated a relationship between the ENSO versus precipitation and stream flow (e.g. Redmond and Koch, 1991; Eltahir, 1996; Chiew *et al*., 1998; Kawamura *et al*., 1998, 2001a,b; Berri and Flamenco, 1999; Simpson and Colodner, 1999; Mosley, 2000). Two different indices, sea-surface temperature (SST) and the Southern Oscillation Index (SOI), are usually used to quantify ENSO. El Niño events, occurring every 2–7 years, are associated with high SST and low SOI anomalies. Conversely, La Niña events are episodes of low SST and high SOI anomalies (Amarasekera *et al*., 1997).

Precipitation is one of the key variables driving various hydrological processes, it is useful to examine the relationship between ENSO and precipitation records to understand climate dynamics (Rajagopalan and Lall, 1998). For example, Dracup and Kahya (1994) examined the relationship between the ENSO and precipitation in North America and showed that precipitation anomalies associated with La Niña are opposite in sign to El

* Correspondence to: Z. X. Xu, Institute of Materials and Environmental Technology, Graduate School, Yamanashi University, Takeda 4-3-11, Kofu 400-8511, Japan. E-mail: xu@mail.yamanashi.ac.jp

Received 26 April 2002
Accepted 3 February 2003

Niño precipitation anomalies. A negative correlation was observed between the eastern equatorial Pacific SST anomalies and seasonal monsoon precipitation over India and Sri Lanka by Amarasekera *et al*. (1997), and the dependence of precipitation variance on the magnitude of the SOI values was observed by McKerchar *et al*. (1998). Kane (1999) checked the association between El Niño and droughts in South Asia and China and found that Singapore, Brunei, Indonesia and East Asia showed a good association, Thailand, Malaysia and most part of the Philippines showed some association, but the north-west Philippines showed opposite results. Gutiérrez and Dracup (2001) investigated the relationship between ENSO events and precipitation in Pacific Rim countries. Wang *et al*. (2000) investigated the teleconnection between the central Pacific and eastern Asia during the extreme phases of ENSO cycles and found that noticeable positive precipitation anomalies occur along the east Asia polar front from southern China via the east China Sea to the Kuroshio extension region during winter and the following spring and early summer. Lau and Wu (2001) investigated the regional processes affecting Asian summer monsoon rainfall variability and the ENSO-related basin-scale SSTs accounted for about 30% of the variability. The interannual variability of summer precipitation over the Eastern Tibetan Plateau (ETP) was examined in relation to the Northern Hemisphere macroscale circulation patterns and the dominant spatial pattern found is a seesaw structure between the southern and northern parts of ETP (Liu and Yin, 2001). Giannini *et al*. (2001) observed that the link between the Southern Oscillation and North Atlantic sea-level pressure was stronger during the 1960s and 1970s and weaker during the earlier part of the century, and the North Atlantic oscillation (NAO) can at times be in phase, at other times out of phase with ENSO. Barlow *et al*. (2002) investigated the drought in central and south-west Asia and found that the regional out-of-phase precipitation relationship is related to large-scale climate variability through a subset of ENSO events characterized by an enhanced signal in the warm pool region of the western Pacific Ocean. Recently, the ENSO has been linked to the development of physically based distributed hydrological models. The relationship between ENSO phenomenon and simulated runoff variability is introduced as a valuable source of information to identify model hypotheses by Wooldridge *et al*. (2002). Recent studies also have indicated that ENSO events can be predicted accurately 1–2 years in advance using a physical model of the coupled ocean–atmosphere system (Amarasekera *et al*., 1997). The ability to predict precipitation, therefore, potentially could be enhanced if a strong relationship between precipitation and ENSO can be quantified.

The principal objective of this study is to identify whether there is any relationship between SOI and precipitation anomalies in South-east Asia and the Pacific region. If the statistical test can result in the detection of a regionally consistent and physically plausible correlation, it may lead to important developments in water resources management for providing the possibility to perform precipitation forecasts conditioned on the past records of the SOI. Most of the previous studies stated above are usually simply investigating the historical records for subtle changes in precipitation patterns, and using the conventional correlation coefficient to examine a statistical relationship between ENSO versus precipitation. In this paper, in addition to parametric and non-parametric tests, the cross-spectral technique is used to examine the cross-correlation between seasonal SOI and precipitation anomalies in the study area. A brief description of the technique used in this study is provided in the next section. The data sets are then outlined. Results from the analysis are summarized and discussed in the last section.

TECHNIQUE DESCRIPTION

Techniques to investigate ENSO effects on precipitation usually include:

1. identifying the difference in precipitation between years classified as ENSO or non-ENSO (Chiew *et al*., 1998; Kane, 2001);
2. statistically testing for correlation between precipitation versus an ENSO index such as SST or SOI (Giannini *et al*., 2001; Waylen and Poveda, 2002);
3. regression analysis between precipitation and SST or SOI (McKerchar *et al*., 1998).

The first part of this study will be mainly on the cross-correlation analysis between SOI and precipitation anomalies in the study area. If a correlation between SOI and precipitation indeed exists, there may be some kind of common cycle between these two time-series. Cross-spectral analysis for estimating coherence between SOI and precipitation anomalies, therefore, is also performed in this study.

Correlation analysis

The correlation coefficient is usually used to measure the degree of association between pairs of random variables. The Pearson correlation coefficient r, especially, is a measure of linear association. The null hypothesis H_0, in which time-series Y are independent and identically distributed normal random variables being not dependent on time-series X, gives the test statistic T_c as

$$T_c = \frac{r\sqrt{n-2}}{\sqrt{1-r^2}} \tag{1}$$

in which r is the correlation coefficient between time-series X and Y, and n is the number of samples. The null hypothesis H_0 is rejected if $|T_c| > T_{1-\alpha/2,\nu}$, where $T_{1-\alpha/2,\nu}$ is the point on the Student's t distribution with $\nu = n-2$ degrees of freedom that has a probability of exceedance of $\alpha/2$.

It is generally difficult to satisfy the condition that a hydrological variable is an independent, identically distributed normal random variable. In this case, the robust distribution-free rank correlation may be more efficient with high power (Kendall, 1975). Kendall's rank coefficient, τ, is an alternative measure of correlation. The hypothesis of no correlation (independence) is performed by estimating rank coefficient τ_a or τ_b (τ_b handles ties) on the basis of the Kendall sum S. Each pair (x_i, y_i) is compared with every other pair (x_j, y_j) $(i, j = 1, 2, \ldots, n)$. The Kendall sum is calculated as $S = P - M$, in which P is the number of cases where $y_i > y_j$ $(i > j)$, and M the number of cases where $y_i < y_j$ $(i > j)$. The statistic, τ_a, is estimated as

$$\tau_a = \frac{S}{n(n-1)/2} \tag{2}$$

If there are n_x sets of ties in the x rankings and the ith set consists of t_i observations $(i = 1, 2, \ldots, n_x)$, and n_y sets of ties in the y rankings and the ith set consists of s_i observations $(i = 1, 2, \ldots, n_y)$, statistic τ_b should be used, and is estimated as follows (Lloyd, 1984)

$$\tau_b = \frac{2S}{\sqrt{\left\{n(n-1) - \sum_{i=1}^{n_x} t_i(t_i-1)\right\}\left\{n(n-1) - \sum_{i=1}^{n_y} s_i(s_i-1)\right\}}} \tag{3}$$

As with the Pearson correlation coefficient, τ_a and τ_b can take on values only between -1 and 1, where the sign indicates the slope of the relationship, and the absolute value indicates the strength of the relationship. For large n, the test is performed using a statistic of the normal approximation Z_c (Kendall, 1962)

$$Z_c = \frac{S}{\sqrt{\mathrm{Var}(S)}} \tag{4}$$

in which

$$\mathrm{var}[S] = \frac{n(n-1)(2n+5) - \sum_x t_i(t_i-1)(2t_i+5) - \sum_y s_i(s_i-1)(2s_i+5)}{18} + \frac{\left[\sum_x t_i(t_i-1)(t_i-2)\right] \times \left[\sum_y s_i(s_i-1)(s_i-2)\right]}{9n(n-1)(n-2)} + \frac{\left[\sum_x t_i(t_i-1)\right] \times \left[\sum_y s_i(s_i-1)\right]}{2n(n-1)} \tag{5}$$

The null hypothesis is rejected at significant level α if $|Z_c| > Z_{(1-\alpha/2)}$, where $Z_{(1-\alpha/2)}$ is the value of the standard normal distribution with a probability of exceedance of $\alpha/2$, and α is the significance level of the test ($\alpha = 0{\cdot}05$).

Coherence analysis

Coherence has been used previously in harmonics analysis and is not a new concept. For example, Kahya and Dracup (1993) defined coherence as

$$\text{coherence} = \mathbf{V}/S \tag{6}$$

in which $\mathbf{V}$ is the vector mean, the magnitude of the vector sum divided by the total number of vectors, and S is the scalar mean, which is the arithmetic mean of the magnitudes of the vectors. In other words, coherence is the scalar sum divided by the total number of vectors. The coherence of a set of vectors is zero when they have the same average magnitude in all directions and is one when they have exactly the same direction. If the coherence is equal to or larger than 0·80, that region is said to be a candidate region.

Spectral analysis is a useful technique for identifying temporal cycles embedded in hydrological processes and has been used by hydrologists for low-frequency analyses (e.g. Lall and Mann, 1995; Shun and Duffy, 1999; Fleming, *et al*., 2002). Cross-spectral and coherence analysis, which may be unfamiliar for some hydrologists, is a quite efficient tool for examining the correlation relationships between pairs of hydrological variables. Both will be outlined in this section. Details for relevant concepts and estimation methods may be found in Hamilton (1994). Given variables X and Y, the cross-spectrum from Y to X is defined as

$$s_{XY}(\varpi) = \frac{1}{2\pi} \sum_{t=-\infty}^{\infty} \gamma_{XY}^{(k)} \{\cos(\varpi k) - i \times \sin(\varpi k)\} \tag{7}$$

in which $\gamma_{XY}^{(k)}$ is the covariance between the value of X and the value that Y assumed k periods earlier (lag k). Cross-spectrum can also be written in terms of its real and imaginary components as

$$s_{XY}(\varpi) = c_{XY}(\varpi) + i \times q_{XY}(\varpi) \tag{8}$$

The real component of the cross-spectrum $c_{XY}(\varpi)$ is known as the co-spectrum between X and Y, and may be interpreted as the portion of the covariance between X and Y that is attributable to cycles with frequency ϖ. Similarly, the imaginary component of the cross spectrum $q_{XY}(\varpi)$ is known as the quadrature spectrum from X to Y.

The coherence $h_{XY}(\varpi)$ between X and Y is defined as a measure of the degree to which X and Y are jointly influenced by cycles of frequency ϖ (Hamilton, 1994). It combines the influences of the co-spectrum and the quadrature spectrum, and is given as

$$h_{XY}(\varpi) = \begin{cases} \dfrac{\{[c_{XY}(\varpi)]^2 + [q_{XY}(\varpi)]^2\}^{1/2}}{\sqrt{s_{YY}(\varpi) s_{XX}(\varpi)}}, & s_{XX}(\varpi) \neq 0,\ s_{YY}(\varpi) \neq 0 \\ 0, & s_{XX}(\varpi) = 0 \text{ or } s_{YY}(\varpi) = 0 \end{cases} \tag{9}$$

It can be shown that $0 \leq h_{XY}(\varpi) \leq 1$ for all ϖ so long as X and Y are covariance-stationary with absolutely summable autocovariance matrics (Fuller, 1976).

For a given frequency ω, the coherence $h_{XY}(\varpi)$ lies between zero and one, inclusive, and reflects the linear relationship between the random coefficients. If $h_{XY}(\varpi)$ is large, this indicates that X and Y have important cycles of frequency in common. For observed samples of n observations denoted $x_1, x_2, \ldots, x_n$, and $y_1, y_2, \ldots, y_n$, the centred and padded data length of N which equals the sum of n and the number of zeros used to pad each centred time-series is defined as

$$\tilde{X}_t = \begin{cases} X_t - \hat{\mu}, & t = 1, 2, \ldots, n \\ 0, & t = (n+1), (n+2), \ldots, N \end{cases} \tag{10}$$

Centring the data simplifies the formulae for estimation of the periodogram and spectral density. The addition of n_0 zeros to the end of the data is called padding. This procedure increases the effective length of the data from n to N in an effort to:

1. increase the computational efficiency of the Fourier transformation of the series;
2. obtain the periodogram ordinates required to give the exact expression of the sample autocovariances in terms of the inverse Fourier transformation of the periodogram;
3. produce periodogram ordinates over a more refined range of frequencies.

Then the cospectrum $\hat{c}_{XY}(\varpi)$ and quadrature spectrum $\hat{q}_{XY}(\varpi)$ are estimated as follows

$$\hat{c}_{XY}(\varpi) = \frac{2\pi}{N} \sum_{t=-[N/2]}^{[N/2]} \varphi\{I_{XY}(\varpi_k)\} w_n(\varpi - \varpi_k) \tag{11}$$

$$\hat{q}_{XY}(\varpi) = \frac{2\pi}{N} \sum_{t=-\lfloor N/2 \rfloor}^{\lfloor N/2 \rfloor} \psi\{I_{XY}(\varpi_k)\} w_n(\varpi - \varpi_k) \tag{12}$$

where $I_{XY}(\varpi_k)$ is the sample cross-periodogram from x to y at frequency ϖ_k expressed as

$$I_{XY}(\varpi_k) = \varphi\{I_{XY}(\omega_k)\} + i\psi_{XY}\{I_{XY}(\omega_k)\} \tag{13}$$

in which

$$\varphi\{I_{XY}(\varpi_k)\} = A_X(\varpi_k)A_Y(\varpi_k) + B_X(\varpi_k)B_Y(\varpi_k) \tag{14}$$

$$\psi\{I_{XY}(\varpi_k)\} = A_X(\varpi_k)B_Y(\varpi_k) - B_X(\varpi_k)A_Y(\varpi_k) \tag{15}$$

where $\varphi\{I_{XY}(\varpi_k)\}$ represents the 'raw' sample cospectrum and $\psi\{I_{XY}(\varpi_k)\}$ represents the 'raw' sample quadrature spectrum. In which $A_X(\varpi_k)$, $B_X(\varpi_k)$, $A_Y(\varpi_k)$ and $B_Y(\varpi_k)$ are coefficients and estimated as

$$A_X(\varpi_k) = \zeta^{1/2} \sum_{i=1}^{N} x_i \cos(\varpi_k i) \tag{16}$$

$$B_X(\varpi_k) = \zeta^{1/2} \sum_{i=1}^{N} x_i \sin(\varpi_k i) \tag{17}$$

$$A_Y(\varpi_k) = \zeta^{1/2} \sum_{i=1}^{N} y_i \cos(\varpi_k i) \tag{18}$$

$$B_Y(\varpi_k) = \zeta^{1/2} \sum_{i=1}^{N} y_i \sin(\varpi_k i) \tag{19}$$

in which ζ is the scale factor equal to $1/(2\pi n)$, and $w_n(\varpi - \varpi_n)$ is the spectral window. Examples of spectral windows include modified Bartlett, Daniell, Tukey, Parzen and Bartlett–Priestley functions. In this paper, the Bartlett–Priestley window function with less bias is used. It is in the following form

$$w_n(\theta) = \begin{cases} \frac{3M}{4\pi} \left\{ 1 - \left(\frac{M\theta}{\pi} \right)^2 \right\}, & |\theta| \le \pi/M \\ 0, & |\theta| > \pi/M \end{cases} \tag{20}$$

in which M is the window parameter and is inversely proportional to the bandwidth of the spectral window. It is usually selected as the last lag at which the estimated autocorrelation function is significantly different from zero. Peaks in a graphical plot of the periodogram indicate frequencies that are present in, and make a significant contribution to, the signal.

DATA DESCRIPTION AND ANALYSIS

In order to investigate the relationship between ENSO episodes and precipitation anomalies, several elements must be determined.

1. Which time period of the ENSO and precipitation has the best correlation: monthly, seasonal, or annual values?
2. What the lead-time or lag is for this correlation?

According to Redmond and Koch (1991), higher time resolution such as 3 months or longer may be desirable. This paper, therefore, will be mainly on the investigation for the correlation between SOI and 3-month precipitation in South-east Asia and the Pacific region.

The index used to characterize the ENSO phenomenon at the present stage of this study is the Southern Oscillation Index (SOI), estimated by the Australian National Climate Centre and the data series was obtained from the Centre's web site. It is widely used to depict the ENSO variation in South-east Asia and the Pacific region. The SOI is estimated from the monthly or seasonal fluctuations in the air pressure difference between Tahiti (approximately 150 °W, 18 °S) and Darwin (approximately 130 °E, 13 °S). Although there are several methods to calculate the SOI values, the difference among these methods, however, has been proved to be very small (Kawamura *et al*., 1998). The method used in this study is the Troup SOI, which is the standardized anomaly of the mean sea-level pressure (MSLP) difference between Tahiti and Darwin and expressed as follows

$$\mathrm{SOI} = 10 \times \frac{D_{\mathrm{MSLP}} - \overline{D}_{\mathrm{MSLP}}}{S_{\mathrm{MSLP}}} \tag{21}$$

in which D_{MSLP} is the difference between the average annual MSLP at Tahiti and Darwin; $\overline{D}_{\mathrm{MSLP}}$ the mean value of the D_{MSLP} over the period 1951 to 1981; and S_{MSLP} the standard deviation of the D_{MSLP} over the same period.

The South-east Asia and Pacific region exhibits a broad range of climatic behaviour. Monthly precipitation data from 30 basins throughout the South-east Asia and Pacific region, collected by Asian Pacific FRIEND member countries and represented in the Catalogue of Rivers for southeast Asia and the Pacific (Flow Regimes from International Experimental and Network Data) as shown in Figure 1, are used (Takeuchi *et al*., 1995; Jayawardena *et al*., 1997; Hidayat *et al*., 2000). According to the regulation predetermined in AP FRIEND, member countries provide their precipitation and discharge data for storage in the database and are solely responsible for the quality of these data. The data extracted from the database and used throughout the analysis are the monthly precipitation from which seasonal values are estimated. The precipitation statistics from 30 representative rain gauges in these basins are given in Table I. The length of record ranges from 24 to 102 years, with an average of 42 years. The catchment areas range from 26 to 130 000 km^2, with an average of 15 587 km^2, and the annual precipitation ranges from 272 mm to 3141 mm, with an average of 1455 mm. The 30 rivers are considered to be capable of representing a wide range of hydrological/climatic districts in the study area.

The World Meteorological Organization (WMO) presently uses the period 1961–1990 as climatological normal for some 4000 stations in 130 countries. It is, therefore, important to conduct a detailed study of the variability of precipitation for this time period and the period 1961–1990 becomes the first 30-year period that has been considered as the standard or baseline for comparison for many different purposes in climatological

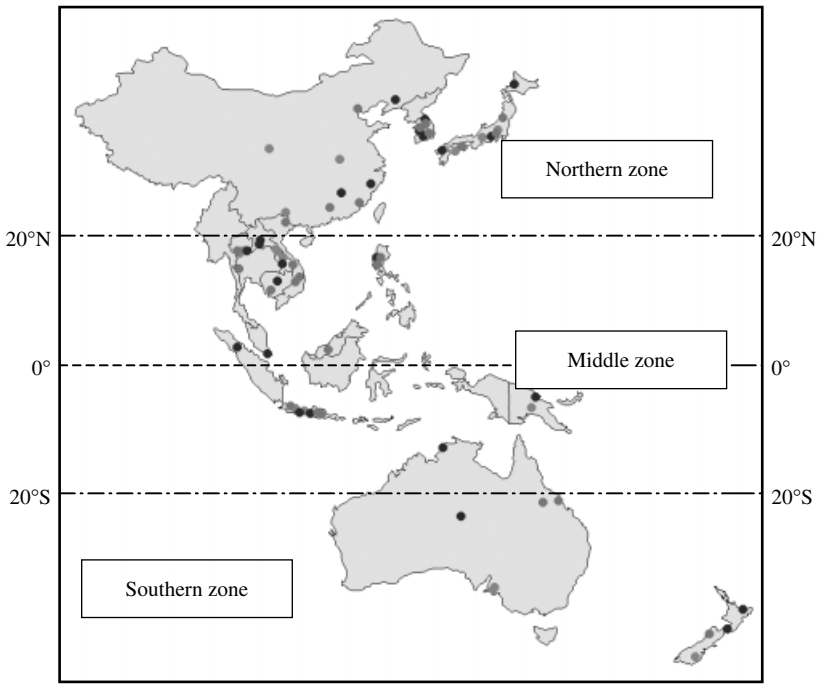

Figure 1. Study area showing the gauge stations

investigations (Liu and Yin, 2001). For comparison, the normalized anomaly of monthly precipitation is estimated for each month

$$Z_{ij} = \frac{P_{ij} - \overline{P}_i}{\sigma_i} \tag{22}$$

in which Z_{ij} is the normalized monthly precipitation anomaly of a given station i for month j ($i = 1, 2, \ldots, 30$; $j = 1, 2, \ldots, 12$), P_{ij} is the monthly precipitation of station i for month j, $\overline{P}_i$ is the mean monthly precipitation of station i for the period 1961–1990, and σ_i is the standard deviation of monthly precipitation of station i during this period.

Data analysis

In order to investigate the relationship between ENSO episodes and precipitation, the precipitation data were split into three categories based on the monthly averaged SOI values. Statistics for each basin are estimated for the entire period, El Niño periods, neutral periods and La Niña periods. Table II lists those results. It clearly shows the tendency that the average monthly precipitation in El Niño periods is small compared with values of both neutral and La Niña periods in parts of southern zone such as Australia and Indonesia. In contrast, the coefficient of variation shows the opposite tendency in the same region, which means that the southern zone may experience dry climate with large variability of precipitation during El Niño periods. With a more detailed examination on the original data for the two rivers in Australia, an interesting fact was found. There are 684 months of data record for Todd River and 816 months for Burdekin River. Both El Niño and La Niña precipitation occurred with approximately same frequencies for the two rivers. El Niño precipitation occurred 213 times at Todd River and 241 times at Burdekin River, and the corresponding frequencies are 31·1% for Todd River and 29·5% for Burdekin River. The La Niña precipitation occurred 203 times at Todd River and 240 times at Burdekin River, and the frequencies are 29·7% and 29·4%, respectively. In other words, both El Niño and La Niña episodes seem to appear with nearly the same probabilities. However, the number of

Table I. Statistics for the river basins and annual precipitation: Cv, coefficient of variation

Country	River	Basin area (km^2)	Data period	Precipitation	Cv
Australia	Burdekin River	130 000	1930–1997	655·87	0·42
	Pioneer River	1500	1930–1997	1676·54	0·40
	Todd River	445	1941–1997	271·54	0·52
	East Finniss River	71	1948–1993	1539·17	0·23
	Torrens River	26	1930–1993	662·24	0·24
	Scott Creek	27	1930–1963	1187·99	0·18
	Scott Creek	27	1968–1998	1025·32	0·22
China	Bei-jiang	46 710	1950–1984	1545·02	0·17
	Jin-jiang	5629	1958–1982	1389·41	0·23
	Jiyun-He	10 288	1957–1980	695·10	0·27
	Gan-jiang	82 015	1956–1985	1542·17	0·21
	Taizi-He	13 883	1955–1985	733·70	0·20
	Ou-jiang	17 859	1960–1985	1633·18	0·21
Indonesia	Citarum	6080	1950–1987	1959·14	0·22
	Bengawan Solo	16 100	1952–1991	1625·38	0·27
	Kali Brantas	12 000	1954–1983	2080·04	0·22
	Citanduy	4460	1970–1993	3140·88	0·21
	Kali-Progo	2380	1971–1995	1961·68	0·22
Japan	Chikugo-gawa	2860	1945–1995	1876·62	0·20
	Fuji-kawa	3570	1949–1993	1123·19	0·19
	Ishikari-gawa	14 330	1889–1990	1092·15	0·15
	Shimanto-gawa	2270	1952–1996	1408·98	0·29
	Shonai-gawa	1010	1941–1996	1539·22	0·16
	Watarase-gawa	2602	1950–1996	1698·47	0·18
Korea	Nam-gang	3466	1960–1993	1365·05	0·21
	Gap-chun	647	1960–1985	1319·79	0·21
Malaysia	Sungai Johor	2636	1948–1995	2635·95	0·17
Philippines	Ilog Itaas ng Agno	1250	1951–1984	1934·03	0·30
Thailand	Mae Nam Ping	33 898	1951–1992	1427·48	0·15
	Mae Nam Mae Klong	30 837	1951–1992	1081·49	0·21
	Mae Nam Nan	34 331	1951–1992	1262·20	0·15

months with zero precipitation during El Niño and La Niña episodes is dramatically different. For example, the months without precipitation during El Niño episodes are 61 at Todd River and 62 at Burdekin River, representing 31·1% and 29·5% of the El Niño months. However, the months without precipitation during La Niña episodes are only 24 at Todd River and 31 at Burdekin River, representing only 11·8% and 12·9% of the La Niña months, and these ratios are less than half of the values in El Niño periods. This also is why the coefficient of variation during El Niño periods is larger than that in La Niña periods. In other words, El Niño episodes indeed may accompany the driest month (year) in some countries such as Australia and Indonesia, which may not only result in less average precipitation, but also may result in more drought periods without any precipitation.

In order to examine the features in different zones affected by ENSO, the study area is further divided into southern, middle and northern zones with 20 °N and 20 °S latitudes as the dividing lines, as given by Xu *et al.* (2001) and shown in Figure 1. The ratios of monthly precipitation for El Niño, neutral and La Niña periods to the mean precipitation over the entire period are presented in Figure 2. The inverse relationship between precipitation and SOI, as illustrated earlier, is the most obvious one in the southern zone, the middle zone shows less tendency, and this kind of relationship seems not to exist in the northern zone. Figure 3 shows the

Table II. Monthly statistics for precipitation occurred over different periods: Cv, coefficient of variation

Country	River	Entire		El Niño		Neutral		La Niña	
		Mean	Cv	Mean	Cv	Mean	Cv	Mean	Cv
Australia	Burdekin River	54·87	1·51	38·18	1·68	54·28	1·51	72·46	1·33
	Pioneer River	140·17	1·49	98·39	1·66	138·10	1·52	185·02	1·28
	Todd River	22·70	1·65	13·88	2·33	24·26	1·50	29·89	1·40
	East Finniss River	117·72	1·30	94·35	1·38	116·70	1·31	136·48	1·23
	Torrens River	54·86	0·81	50·26	0·83	51·33	0·80	64·24	0·79
	Scott Creek (1)	99·05	0·78	90·12	0·82	96·42	0·76	109·32	0·79
	Scott Creek (2)	85·61	0·81	77·51	0·74	80·38	0·90	102·86	0·75
China	Bei-jiang	128·68	0·82	133·63	0·83	123·38	0·86	131·76	0·77
	Jin-jiang	115·59	1·03	121·74	1·05	114·88	1·07	111·68	0·96
	Jiyun-He	57·93	1·59	58·48	1·41	59·45	1·67	55·49	1·61
	Gan-jiang	128·50	0·86	138·19	0·76	118·51	0·91	134·40	0·89
	Taizi-He	61·17	1·27	59·06	1·16	58·02	1·33	66·70	1·27
	Ou-jiang	136·07	0·80	146·35	0·69	114·91	0·82	156·09	0·81
Indonesia	Citarum	163·48	0·74	149·15	0·91	168·54	0·74	168·68	0·61
	Bengawan Solo	135·62	0·92	116·01	1·17	140·94	0·88	145·45	0·80
	Kali Brantas	173·46	0·77	138·17	1·00	175·15	0·78	196·20	0·62
	Citanduy	163·48	0·74	149·15	0·91	168·54	0·74	168·68	0·61
	Kali-Progo	184·71	0·80	165·32	0·92	196·92	0·75	195·79	0·71
Japan	Chikugo-gawa	156·38	0·89	164·30	0·85	160·71	0·98	142·68	0·79
	Fuji-kawa	93·60	0·77	105·02	0·76	86·00	0·83	92·61	0·70
	Ishikari-gawa	91·06	0·60	90·75	0·61	89·28	0·55	93·36	0·63
	Shimanto-gawa	117·42	1·03	131·61	1·04	113·57	1·07	108·26	0·93
	Shonai-gawa	128·27	0·70	137·87	0·69	121·90	0·75	127·03	0·64
	Watarase-gawa	141·54	0·84	146·37	0·82	132·23	0·87	149·01	0·82
Korea	Nam-gang	113·80	0·90	122·39	0·93	108·12	0·90	112·15	0·87
	Gap-chun	109·90	1·03	111·12	0·97	106·77	1·08	113·11	1·02
Malaysia	Sungai Johor	218·73	0·55	210·08	0·59	230·54	0·50	211·24	0·59
Philippines	Ilog Itaas ng Agno	161·19	1·17	164·71	1·19	158·96	1·19	161·46	1·14
Thailand	Mae Nam Ping	118·96	1·04	116·41	1·03	113·33	1·02	128·88	1·07
	Mae Nam Klong	90·12	1·04	83·53	1·05	89·33	1·10	97·32	0·96
	Mae Nam Nan	105·18	1·01	105·52	0·94	102·24	1·02	108·83	1·05

same plot for the coefficient of variation. It is easily understood that the relationship between precipitation and SOI for variation is opposite to that for average precipitation in the study area. In other words, precipitation in El Niño periods shows the largest variation and precipitation in La Niña periods shows the smallest variation. This tendency is strong in the southern zone, becomes weak in the middle zone and disappears in the northern zone of the study area.

In the southern zone, the average monthly precipitation during El Niño periods is less than 20% of that over the entire period, but the coefficient of variation is greater by nearly 10% of that over the entire period. In contrast, the average monthly precipitation over La Niña periods is greater than 23% and the coefficient of variation is less than 8% compared with the values over the entire period. The monthly precipitation and the coefficient of variation during neutral periods are approximately equal to the values during the entire period. In the middle zone, this kind of tendency is also exhibited. The average monthly precipitation and the coefficient of variation during El Niño periods are less than 8% and greater than 12% of the values over the entire period, respectively. The average monthly precipitation and coefficient of variation during La Niña periods are greater than 5% and less than 8% compared with the values over the entire period. However, this tendency

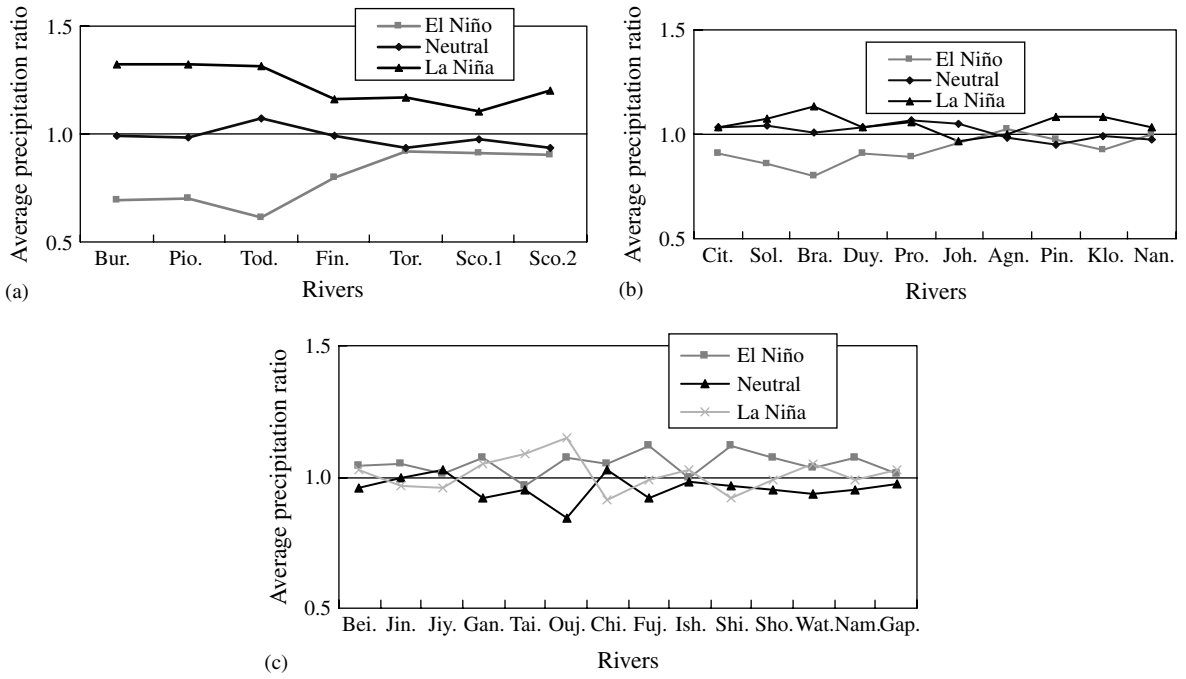

Figure 2. Precipitation ratios in the different climatic zones (original time-series): (a) southern zone (rivers in Australia, Table I), (b) middle zone (rivers in Indonesia, Malaysia, Philippines and Thailand, Table I) and (c) northern zone (rivers in China, Japan and Korea, Table I)

completely disappears in the northern zone, as shown in Figure 4. In other words, monthly precipitation is generally smaller and variation is usually larger for El Niño precipitation as compared with that in La Niña episodes, and even in neutral episodes in southern and central regions. This dependency is greater for the basins in Australia, smaller in Indonesia, Philippines, Thailand and Malaysia, and disappears for most of the basins in China, Japan, and Korea. The plots, given in Figure 4, also show that characteristically both the average monthly precipitation and the variance of precipitation in China and Japan do not show any clear tendency over El Niño and La Niña episodes.

In summary, in the southern zone of the study area including Australia and Indonesia, rivers tend to have opposite response during El Niño and La Niña episodes. Responses in the middle zone are less clear, and this tendency disappears in the northern zone of the study area. In other words, the analysis shows that the southern and middle zones in the study area tend to be more associated with El Niño events than the northern zone.

RESULT ANALYSIS AND DISCUSSIONS

The main objective of this study was to investigate the type and magnitude of the correlation that may exist between the SOI and precipitation in the study area. Similar to McKerchar *et al*. (1998), Chiew *et al*. (1998) and Cluis and Laberge (2002), El Niño and La Niña months are strictly identified by smoothing the monthly SOI values at six months, with smoothed SOI values lower than $-5{\cdot}0$ or higher than $+5{\cdot}0$, respectively. Other months with values of SOI between $-5{\cdot}0$ and $+5{\cdot}0$ are defined as neutral months.

Correlation between SOI and precipitation anomalies

In order to examine the relationship between the SOI and precipitation, correlation coefficients between the 3-month running SOI averages and precipitation anomalies are estimated. Because the ENSO typically has a

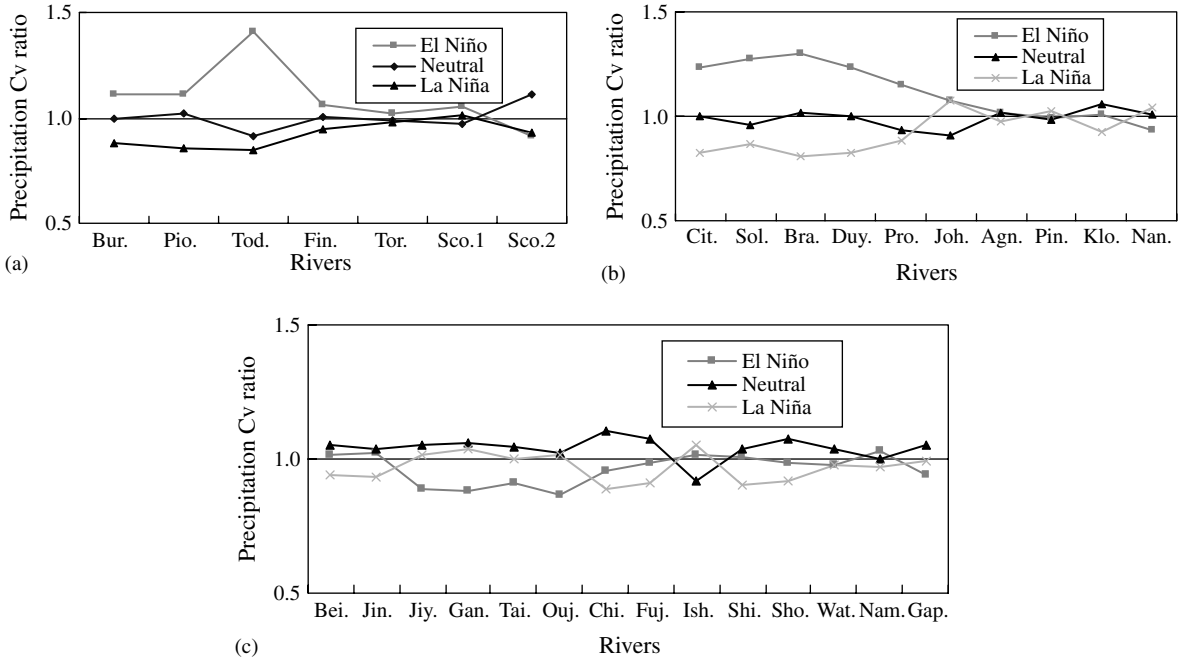

Figure 3. Precipitation coefficient of variation (Cv) ratios in the different climatic zones (original time-series): (a) southern zone (rivers in Australia, Table I), (b) middle zone (rivers in Indonesia, Malaysia, Philippines and Thailand, Table I) and (c) northern zone (rivers in China, Japan and Korea, Table I)

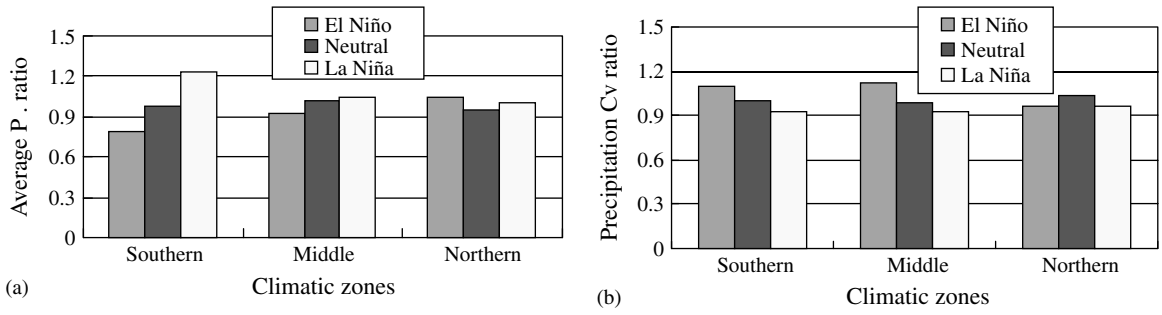

Figure 4. Average precipitation ratio (previous time-series): average precipitation and precipitation coefficient of variation (Cv)

nearly periodic behaviour with high- (2–3 years) and low-frequency (4–7 years) bands (Lall and Mann, 1995), lags from 0 to 30 (7 years) seasons are estimated in this study. A lag of zero defines that the ENSO event and the precipitation period end in the same month; a lag of 1 defines the ENSO period ends 3 months before the precipitation period, and so on. The lag correlation between SOI and precipitation anomalies is estimated using both parametric and non-parametric methods. Lag-0 to lag-30 correlation coefficients are estimated, and the largest one among these 31 correlation coefficients is selected. The last column in Table III presents the results of the correlation test at the significance level of 5%. The results indicate that the association between SOI and precipitation anomalies are significant in nearly all basins in Australia and Indonesia (generally greater than 0·2). The association is also clear in Thailand, but most of the cross-correlations are statistically insignificant in other countries. Both the Pearson correlation coefficient and the non-parametric Mann–Kendall test show the same results. Table IV further shows the largest lag-k cross-correlation between the SOI and precipitation

Table III. Test results for cross-correlation between SOI and precipitation

Country	River	r_c	τ_a/τ_b	R/A[a]
Australia	Burdekin River	0·425	0·263	R
	Pioneer River	0·335	0·213	R
	Todd River	0·273	0·122	R
	East Finniss River	0·254	0·193	R
	Torrens River	0·202	0·150	R
	Scott Creek (1)	0·015	0·029	A
	Scott Creek (2)	0·256	0·192	R
China	Bei-jiang	0·071	0·052	A
	Jin-jiang	0·014	0·009	A
	Jiyun-He	−0·125	−0·074	A
	Gan-jiang	−0·010	−0·065	A
	Taizi-He	0·137	0·130	A(R)
	Ou-jiang	−0·039	−0·035	A
Indonesia	Citarum	0·234	0·177	R
	Bengawan Solo	0·348	0·262	R
	Kali Brantas	0·436	0·318	R
	Citanduy	0·308	0·221	R
	Kali-Progo	0·311	0·246	R
Japan	Chikugo-gawa	−0·097	−0·078	A
	Fuji-kawa	−0·064	−0·060	A
	Ishikari-gawa	0·027	0·005	A
	Shimanto-gawa	−0·101	−0·085	A
	Shonai-gawa	0·009	−0·038	A
	Watarase-gawa	−0·008	−0·033	A
Korea	Nam-gang	−0·004	−0·016	A
	Gap-chun	0·094	0·025	A
Malaysia	Sungai Johor	−0·004	−0·023	A
Philippines	Ilog Itaas ng Agno	0·041	−0·001	A
Thailand	Mae Nam Ping	0·157	0·083	R(A)
	Mae Nam Mae Klong	0·258	0·110	R
	Mae Nam Nan	0·084	0·046	A

[a] R, reject hypothesis H_0; A, accept hypothesis H_0.

anomalies, among the correlation coefficients from lag-1 to lag-30. These coefficients are generally greater than 0·2 in most of the basins. The correlation is obvious in the study area, with several basins showing lag-k correlation greater than 0·3. The precipitation in the southern part of the study area appears to be more strongly correlated with the SOI at smaller lags compared with that in the northern part of the study area.

On the basis of the preliminary results from correlation analysis, several conclusions may be drawn.

1. There is a clear correlation between El Niño–Southern Oscillation and the precipitation anomalies in most basins of the study area. Significant correlations are found in nearly all river basins in Australia, Indonesia and Thailand.
2. In general, the precipitation associated with warm ENSO events (El Niño) tend to be below-normal with a larger range of variation, and those associated with cold events (La Niña) tend to be above-normal with a smaller variation range. This tendency is clear in the southern part of the study area, is weak in the middle zone, but disappears in northern zone.

Table IV. Largest correlation coefficients between SOI and precipitation

Country	River	Correlation	
		Lag	*r*
Australia	Burdekin River	1	0·349
	Pioneer River	1	0·249
	Todd River	1	0·190
	East Finniss River	8	−0·315
	Torrens River	15	0·209
	Scott Creek (1)	21	−0·236
	Scott Creek (2)	12	0·152
China	Bei-jiang	3	0·252
	Jin-jiang	11	−0·243
	Jiyun-He	3	−0·379
	Gan-jiang	8	0·238
	Taizi-He	25	0·099
	Ou-jiang	6	0·303
Indonesia	Citarum	27	−0·150
	Bengawan Solo	1	0·260
	Kali Brantas	1	0·229
	Citanduy	4	−0·326
	Kali-Progo	25	−0·248
Japan	Chikugo-gawa	4	0·185
	Fuji-kawa	14	0·201
	Ishikari-gawa	22	0·106
	Shimanto-gawa	5	0·224
	Shonai-gawa	4	0·246
	Watarase-gawa	5	0·216
Korea	Nam-gang	11	−0·245
	Gap-chun	11	0·325
Malaysia	Sungai Johor	3	−0·215
Philippines	Ilog Itaas ng Agno	18	0·238
Thailand	Mae Nam Ping	21	−0·180
	Mae Nam Mae Klong	1	0·215
	Mae Nam Nan	7	0·227

3. The so-called most frequent lag with largest correlation coefficient was not obvious in the study area. The lags with greatest correlation coefficient are considerably variable. Although Woolhiser *et al*. (1993) found that the most frequent lag in south-western USA was about 3 months with the SOI leading precipitation, and strong correlations were also found for lag periods between 4 and 6 months in Colombia by Gutiérrez and Dracup (2001), similar regulation seems not exist in South-east Asia and the Pacific region.

In summary, the analysis shows that precipitation responses during El Niño and La Niña episodes are indeed not equal and opposite in some basins of the study area, especially those in the response of southern zone. There is, however, a substantial variation in the response of precipitation anomalies to El Niño or La Niña episodes over different climatic zones.

Coherence analysis

The main practical benefit of the coherence analysis is to reveal the linear relationship inherent in two time-series that easily could have been overlooked, or to provide semi-quantitative confirmation of certain

properties that might have been inferred visibly. These include both annual and semi-annual hydrological cycles, and the confirmation of the relationship between precipitation anomalies and SOI time-series.

The results of the previous section demonstrate that there are some kinds of associations between SOI and precipitation anomalies in the study area. Previous studies have shown that the SOI has nearly periodic behaviour with high- (2–3 years) and low-frequency (4–7 years) bands corresponding to ENSO, which is understood as an internal self-sustained equatorial oscillation in the coupled ocean–atmosphere system (Lall and Mann, 1995). If this is true, there may be some kind of coherent relationship between SOI and the periodic hydrological processes. Of interest to the hydrologists is how the ENSO produces variability of precipitation through the hydrological cycle. Although the variation in both ENSO and hydrological processes is random from year to year, a careful examination may reveal some kind of coherent pattern for these two physical processes. The identification of coherence also is relevant to the interpretation of the cross-correlation between ENSO and precipitation anomalies. The results from the cross-spectral and coherence analysis for each basin in the study area are given in Table V. It presents the frequency and cycle with largest coherence between the SOI and precipitation anomalies.

Table V. Largest coherence between SOI and precipitation

Country	River	Maximum coherence		
		Frequency	Cycle	Coherence
Australia	Burdekin River	0·032	31	0·298
	Pioneer River	0·500	2	0·142
	Todd River	0·170	6	0·280
	East Finniss River	0·025	40	0·381
	Torrens River	0·007	133	0·171
	Scott Creek (1)	0·015	67	0·055
	Scott Creek (2)	0·015	67	0·529
China	Bei-jiang	0·500	2	0·112
	Jin-jiang	0·018	57	0·221
	Jiyun-He	0·325	3	0·724
	Gan-jiang	0·260	4	0·428
	Taizi-He	0·498	2	0·268
	Ou-jiang	0·155	6	0·633
Indonesia	Citarum	0·485	2	0·067
	Bengawan Solo	0·360	3	0·260
	Kali Brantas	0·500	2	0·243
	Citanduy	0·298	3	0·328
	Kali-Progo	0·093	10	0·274
Japan	Chikugo-gawa	0·370	3	0·295
	Fuji-kawa	0·280	4	0·521
	Ishikari-gawa	0·015	67	0·076
	Shimanto-gawa	0·165	6	0·094
	Shonai-gawa	0·002	400	0·521
	Watarase-gawa	0·120	8	0·011
Korea	Nam-gang	0·002	400	0·311
	Gap-chun	0·123	8	0·021
Malaysia	Sungai Johor	0·500	2	0·216
Philippines	Ilog Itaas ng Agno	0·075	13	0·077
Thailand	Mae Nam Ping	0·005	200	0·527
	Mae Nam Mae Klong	0·010	100	0·541
	Mae Nam Nan	0·065	15	0·181

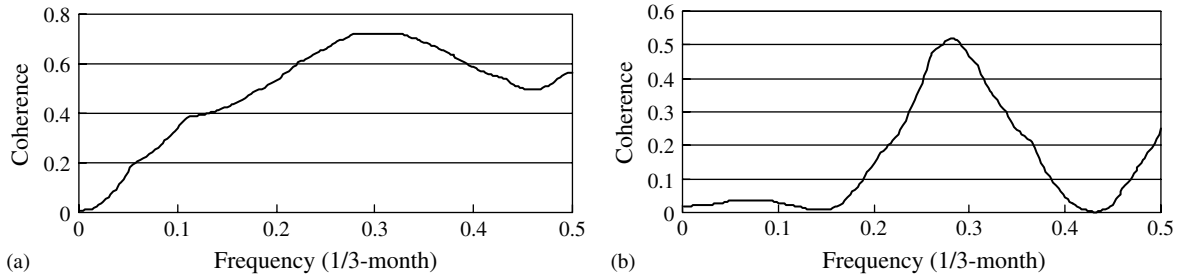

Figure 5. Coherence between precipitation anomalies and SOI: (a) Jiyun River in China and (b) Fuji River in Japan

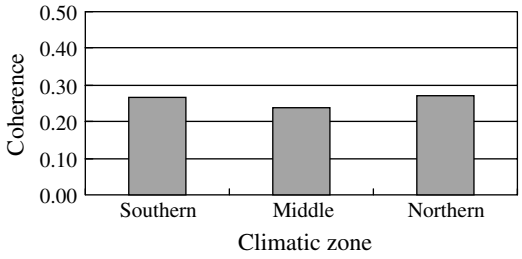

Figure 6. Coherence comparison among three climatic zones

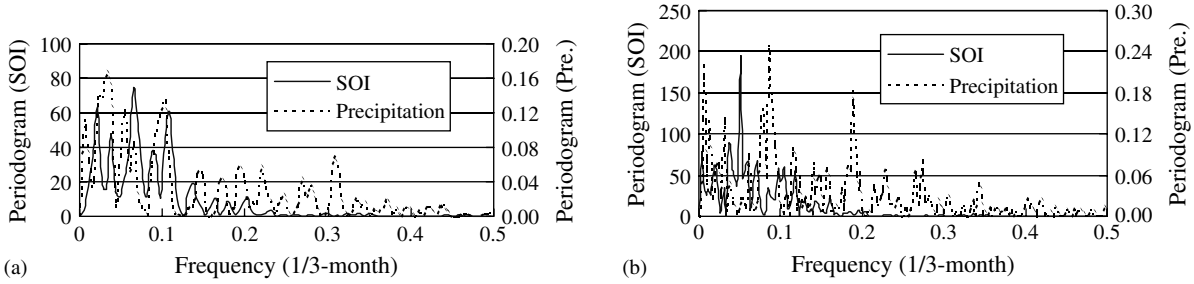

Figure 7. Periodogram comparison between precipitation anomalies and SOI: (a) Jiyun River in China and (b) Fuji River in Japan

With a preliminary display of the coherence output, as presented in Figure 5, it seems that the precipitation anomalies in several basins of the study area show a good coherent relationship with the SOI time-series. From the largest coherence value and the corresponding frequency and cycles given in Table V, it is clear that some precipitation anomalies show the greatest coherence with the SOI at the period from 6 to 12 months, although several coherence peaks have an interdecadal period longer than 12 months. The 6–12 month period may be associated with the interannual SOI cycles. The periods of longer than 1 year may reflect the decadal variability of the precipitation and ENSO.

The comparison among the three zones for the average of the largest coherence is given in Figure 6. It can be seen that the spatial features with respect to the coherence of the precipitation anomalies with the SOI are not apparent. In other words, great variation of coherence is present across the study area.

As the results showed from correlation analysis, the coherence between SOI and precipitation anomalies should have large values, especially in Australia and Indonesia. Conversely, the results presented in Table V do not provide an ideal result as expected previously. In order to investigate whether there is a common cycle between SOI and precipitation anomalies, the periodograms for both SOI and precipitation anomalies presented in Figure 5 are estimated and the results are shown in Figure 7. The periodogram can capture the

portion of the sample variance of the time-series that can be attributed to cycles of different frequencies. It is obvious, even these two basins give two of the largest values of the coherence between SOI and precipitation anomalies, it is indeed that there seems no common cycle for the SOI and precipitation anomalies. From Figure 7, it is seen that the coherence between SOI and precipitation anomalies is not significant, or the same common cycles for SOI and precipitation anomalies in the study area seem not to exist, even in Australia or Indonesia. By this analysis there does not appear to be any common cycles between SOI and precipitation anomalies, although further investigation is required.

CONCLUSIONS

The association between the El Niño–Southern Oscillation and seasonal precipitation anomalies in South-east Asia and the Pacific region were investigated in this study. The analyses show that dry conditions in the southern zone and part of the middle zone of the study area tend to be associated with El Niño, and below-normal seasonal precipitation and above-normal precipitation variation are consistently identified in the El Niño months, and the feature is opposite for La Niña events. El Niño events significantly reduce precipitation in the southern zone of the study area. In contrast, La Niña events cause the precipitation in this area to increase. This is also true for the middle zone, although the tendency is not as strong as that in southern zone. This tendency does not seem to exist in the northern zone. It was found that the basins in southern zone have better correlation with ENSO than the basins in the middle and northern zones. Precipitation anomalies in the northern zone appear to exhibit very little dependence on ENSO. Most of the lag correlations of precipitation against SOI are statistically significant in southern zone but insignificant in northern zone.

Coherence analysis was performed on time-series of precipitation at 30 basins in the study area. Cycles of 6–12 month periods were revealed from the analysis. These cycles, however, do not seem to be the true common cycles for SOI and precipitation anomalies and the common cycle for both does not seem to exist in the study area, although further detailed study is required. On going investigation of the correlation between precipitation anomalies and other ENSO indexes, such as SST and PDO (Pacific Decadal Oscillation), is currently under way. The coherence analysis needs more justification in hydrological studies so as to capture the periodic structure of the observed time-series at given temporal resolutions efficiently.

ACKNOWLEDGEMENT

This study has been financed by Japan Ministry of Education, Culture, Sports, Science and Technology (MEXT) under the project "Model development for prediction of water resources change due to natural variation and human modification in the Asian monsoon region" (RR2002). The authors would like to thank the editor and two anonymous reviewers for their constructive comments and suggestions, which resulted in a significant improvement of the manuscript.

REFERENCES

Amarasekera KN, Lee RF, Williams ER, Eltahir EA. 1997. ENSO and the natural variability in the flow of tropical rivers. *Journal of Hydrology* **200**: 24–39.

Barlow M, Gullen H, Lyon B. 2002. Drought in Central and Southwest Asia: La Niña, the warm pool, and Indian Ocean precipitation. *Journal of Climate* **15**(7): 697–700.

Berri GJ, Flamenco EA. 1999. Seasonal volume forecast of the Diamante River, Argentina, based on El Niño observations and predictions. *Water Resources Research* **35**(12): 3803–3810.

Chiew FHS, Piechota TC, Dracup JA, McMahon TA. 1998. El Niño/Southern Oscillation and Australian rainfall, streamflow and drought: Links and potential for forecasting. *Journal of Hydrology* **204**: 138–149.

Cluis D, Laberge C. 2002. Analysis of the El Niño effect on the discharge of selected rivers in the Asia-Pacific region. *Water International* **27**(2): 279–293.

Dracup JA, Kahya E. 1994. The relationships between U.S. streamflow and La Niña events. *Water Resources Research* **30**(7): 2133–2141.

Eltahir EA. 1996. El Niño and the natural variability in the flow of the Nile River. *Water Resources Research* **32**(1): 131–137.
Fleming SW, Lavenue AM, Aly AH, Adams A. 2002. Practical applications of spectral analysis to hydrologic time series. *Hydrological Processes* **16**: 565–574.
Fuller WA. 1976. *Introduction to Statistical Time Series*. Wiley: New York; 156 pp.
Giannini A, Cane MA, Kushnir Y. 2001. Interdecadal changes in the ENSO teleconnection to the Caribbean region and the North Atlantic oscillation. *Journal of Climate* **14**: 2867–2879.
Gutiérrez F, Dracup JA. 2001. An analysis of the feasibility of long-range streamflow forecasting for Colombia using El Niño–Southern Oscillation indicators. *Journal of Hydrology* **246**: 181–196.
Hamilton JD. 1994. *Time Series Analysis*. Princeton University Press: Princeton, NJ; 799 pp.
Hidayat P, Jayawardena AW, Takeuchi K, Lee S. 2000. *Catalogue of Rivers for Southeast Asia and the Pacific*. Vol. 3. The UNESCO–IHP Regional Steering Committee (RSC) for Southeast Asia and the Pacific: UNESCO Jakarta Office, Jakarta, Indonesia, 268 pp.
Jayawardena AW, Takeuchi K, Machbub B. 1997. *Catalogue of Rivers for Southeast Asia and the Pacific*, Vol. 2. The UNESCO-IHP Regional Steering Committee (RSC) for Southeast Asia and the Pacific: UNESCO Jakarta Office, Jakarta, Indonesia, 285 pp.
Kahya E, Dracup JA. 1993. U.S. streamflow patterns in relation to the El Niño/Southern Oscillation. *Water Resources Research* **29**(8): 2491–2503.
Kane RP. 1999. El Niño timings and rainfall extremes in India, Southeast Asia and China. *International Journal of Climatology* **19**: 653–672.
Kawamura A, McKerchar AI, Spigel RH, Jinno K. 1998. Chaotic characteristics of the Southern Oscillation Index time series. *Journal of Hydrology* **204**: 168–181.
Kawamura A, Eguchi S, Jinno K. 2001a. Correlation between Southern Oscillation and monthly precipitation in Fukuoka. *Journal of Hydraulics and Coastal and Environmental Engineering, Japanese Society of Civil Engineers* **691**(II-57): 153–158 (in Japanese).
Kawamura A, Eguchi S, Jinno K. 2001b. Statistical characteristics of Southern Oscillation Index and its barometric pressure data. *Journal of Hydraulics Engineering, Japanese Society of Civil Engineers* **45**: 169–174 (in Japanese).
Kendall MG. 1962. *Rank Correlation Methods*, Charles Griffin: London; 94–100.
Kendall MG. 1975. *Rank Correlation Measures*. Charles Griffin: London; 202 pp.
Lall U, Mann M. 1995. The Great Salt Lake: a barometer of low-frequency climatic variability. *Water Resources Research* **31**(10): 2503–2515.
Lau KM, Wu HT. 2001. Principal modes of rainfall-SST variability of the Asian summer monsoon: A reassessment of the Monsoon-ENSO relationship. *Journal of Climate* **14**: 2880–2895.
Liu XD, Yin ZY. 2001. Spatial and temporal variation of summer precipitation over the Eastern Tibetan Plateau and the North Atlantic oscillation. *Journal of Climate* **14**: 2896–2909.
Lloyd E. 1984. *Handbook of Applicable Mathematics: Statistics (VI)*. Wiley: Chichester; 1911 pp.
McKerchar AI, Pearson CP, Fitzharris BB. 1998. Dependency of summer lake inflows and precipitation on spring SOI. *Journal of Hydrology* **205**: 66–80.
Mosley MP. 2000. Regional differences in the effects of El Niño and La Niña on low flows and floods. *Hydrological Science Journal* **45**(2): 249–267.
Rajagopalan B, Lall U. 1998. Interannual variability in western US precipitation. *Journal of Hydrology* **210**: 51–67.
Redmond KT, Koch RW. 1991. Surface climate and streamflow variability in western United States and their relationship to large-scale circulation indices. *Water Resources Research* **27**(9): 2381–2399.
Shun TY, Duffy CJ. 1999. Low-frequency oscillations in precipitation, temperature, and runoff on a west facing mountain front: a hydrologic interpretation. *Water Resources Research* **35**(1): 191–201.
Simpson HJ, Colodner DC. 1999. Arizona precipitation response to the Southern Oscillation: A potential water management tool. *Water Resources Research* **35**(12): 3761–3769.
Takeuchi K, Jayawardena AW, Takahasi Y. 1995. *Catalogue of Rivers for Southeast Asia and the Pacific*, Vol. 1. The UNESCO-IHP Regional Steering Committee (RSC) for Southeast Asia and the Pacific: UNESCO Jakarta Office, Jakarta, Indonesia, 291 pp.
Waylen P, Poveda G. 2002. El Niño–Southern Oscillation and aspects of western South American hydrol-climatology. *Hydrological Processes* **16**: 1247–1260.
Wang B, Wu RG, Fu XH. 2000. Pacific–East Asia teleconnection: how does ENSO affect East Asian climate? *Journal of Climate* **13**: 1517–1536.
Wooldridge SA, Kalma JD, Franks SW, Kuczera G. 2002. Model identification by space–time disaggregation: a case study from eastern Australia. *Hydrological Processes* **16**: 459–477.
Woolhiser DA, Keefer TO, Redmond KT. 1993. Southern Oscillation effects on daily precipitation in the southwestern United States. *Water Resources Research* **29**(4): 1287–1295.
Xu ZX, Takeuchi K, Ishidaira H. 2001. Precipitation variation due to climatic change in Southeast Asia and the Pacific region. In *Proceedings of the International Symposium on Achievements of IHP-V in Hydrological Research*, Thuc Tran (ed.). UNESCO Jakarta Office: Ha Noi, Viet Nam; 399–413.

